

## Fermi surface gapping and nesting in the surface phase transition of Sn/Cu(100)

J. Martínez-Blanco,<sup>1</sup> V. Joco,<sup>1</sup> H. Ascolani,<sup>2</sup> A. Tejada,<sup>3</sup> C. Quirós,<sup>4</sup> G. Panaccione,<sup>5</sup> T. Balasubramanian,<sup>6</sup> P. Segovia,<sup>1</sup> and E. G. Michel<sup>1</sup>

<sup>1</sup>Dpto. de Física de la Materia Condensada and Instituto Universitario de Ciencia de Materiales “Nicolás Cabrera,” Universidad Autónoma de Madrid, 28049 Madrid, Spain

<sup>2</sup>CONICET and Centro Atómico Bariloche, Comisión Nacional de Energía Atómica, 8400 Bariloche, Argentina

<sup>3</sup>Matériaux et Phénomènes Quantiques, FR CNRS 2437, Université Paris 7, 75251 Paris, France

<sup>4</sup>Dpto. de Física, Universidad de Oviedo, Avda. Calvo Sotelo s/n, 33007 Oviedo, Spain

<sup>5</sup>Istituto Nazionale per la Fisica della Materia INFN-Lab. TASC, S.S. 14 Km 163.5, in Area Science Park, I-34012 Basovizza, Trieste, Italy

<sup>6</sup>Max-Lab, University of Lund, Box 118, SE-221 00 Lund, Sweden

(Received 25 April 2005; published 14 July 2005)

We identify and characterize a two-dimensional phase transition in a layer of Sn on Cu(100). The stable phase at room temperature has a  $(3\sqrt{2} \times \sqrt{2})R45^\circ$  structure. Above  $\sim 360$  K, a new phase with  $(\sqrt{2} \times \sqrt{2})R45^\circ$  structure is formed. The high-temperature phase exhibits a quasi-two-dimensional free-electron surface band, with Fermi surface nesting in excellent agreement with the three-times larger periodicity of the low-temperature phase. A momentum-dependent band gap opens along the nested areas of the Fermi surface in the low-temperature phase. The phase transition is a clear experimental confirmation of the role of Fermi-surface gapping and nesting in the stabilization of a commensurate two-dimensional phase, which is interpreted as a charge-density wave.

DOI: [10.1103/PhysRevB.72.041401](https://doi.org/10.1103/PhysRevB.72.041401)

PACS number(s): 73.20.At, 68.35.Rh

Two-dimensional (2D) phase transitions triggered by a gain in electronic energy have deserved ample attention during recent years.<sup>1–9</sup> The most important example of this kind is the formation of a charge-density wave (CDW). The CDW state is an easily accessible, macroscopically coherent state with very interesting properties.<sup>10–12</sup> As the CDW sets in, the lattice reorders slightly, giving rise to a periodic lattice distortion (PLD) and a new supercell. The loss of elastic energy is compensated in the new supercell by a gain in electronic energy related to the opening of a band gap  $2W$ . This process is favored when a significant fraction of electrons is affected, i.e., if there are large parallel portions of the Fermi surface separated by  $2k_F$  (nesting). Then, the spatial periodicity of the PLD is  $2\pi/2k_F$  and the nested portions of the Fermi surface are eliminated in the CDW state. The reduced coordination at the surface of a crystal might help CDW stabilization, but due to the complex experimental phenomenology the assignment is difficult and often disputed.<sup>2–6,9</sup> Nakagawa *et al.*<sup>7</sup> have reported that 0.5 monolayers (ML) of In on Cu(100) exhibit a reversible phase transition from a  $(\sqrt{2} \times \sqrt{2})R45^\circ$  phase above  $\sim 350$  K to a charge-ordered  $(9\sqrt{2} \times 2\sqrt{2})R45^\circ$  phase below. While a surface band gap is observed concomitantly with the phase transition, the nesting vector  $2k_F$  does not correspond with the periodicity of the PLD. Thus, the role of Fermi-surface nesting versus other driving forces (like elastic energy) must be analyzed. Our motivation to study Sn/Cu(100) was threefold. First, in view of the properties of In/Cu(100), we considered other adsorbate/substrate combinations that exhibit similar reconstructions. Indeed, it is not clear whether the CDW stabilization is related to the particular band filling and lattice energies of In or is a more general phenomenon. In, Sn, Tl, Pb, and other elements form  $(n\sqrt{2} \times m\sqrt{2})R45^\circ$  reconstructions

when adsorbed on the (100) surfaces of noble metals. Second, it is imperative to test several theoretically derived concepts, including Fermi-surface nesting, which are not evident in the case of In/Cu(100), but seem to play a crucial role in other systems.<sup>9</sup> Finally, the simpler  $(3\sqrt{2} \times \sqrt{2})R45^\circ$  structure of the Sn overlayer could help to understand the relevant energies involved. This idea is supported by the atomic model proposed for this surface,<sup>13</sup> which can be interpreted in terms of a one-dimensional PLD (see also below).

In this paper, we report angle-resolved photoemission spectroscopy (ARPES), low-energy electron diffraction (LEED), and surface x-ray diffraction (SXRD) measurements of 0.5 ML of Sn atoms on Cu(100). The use of ARPES allows us to directly probe the electronic band structure near the Fermi energy, while LEED and SXRD provide structural information. Above  $\sim 360$  K, the surface presents a  $(\sqrt{2} \times \sqrt{2})R45^\circ$  superstructure (in the following,  $\sqrt{2}$ ). A surface free-electron-like band defines a  $2k_F$  nesting vector equal to  $1/3$  of the  $\sqrt{2}$  reciprocal lattice vector. In excellent agreement with this nesting vector, a reversible phase transition to a  $(3\sqrt{2} \times \sqrt{2})R45^\circ$  structure (in the following,  $3\sqrt{2}$ ) is observed at 360 K. The phase transition is associated with the partial gapping of the Fermi surface in areas coinciding with the  $3\sqrt{2}$  zone edge. We discuss the interpretation of this phase transition as the stabilization of a surface CDW.

The experiments are performed using three different ultrahigh vacuum chambers. ARPES experiments use synchrotron light from beamline 33 at MaxLab (Lund, Sweden) and from the APE beamline at Elettra Laboratory (Trieste, Italy).<sup>14</sup> SXRD experiments are done at the ID03 beamline of the European Synchrotron Radiation Facility (Grenoble, France). The  $3\sqrt{2}$  structure is produced by deposition of 0.5 ML of Sn at 300 K. The coverage is calibrated from the

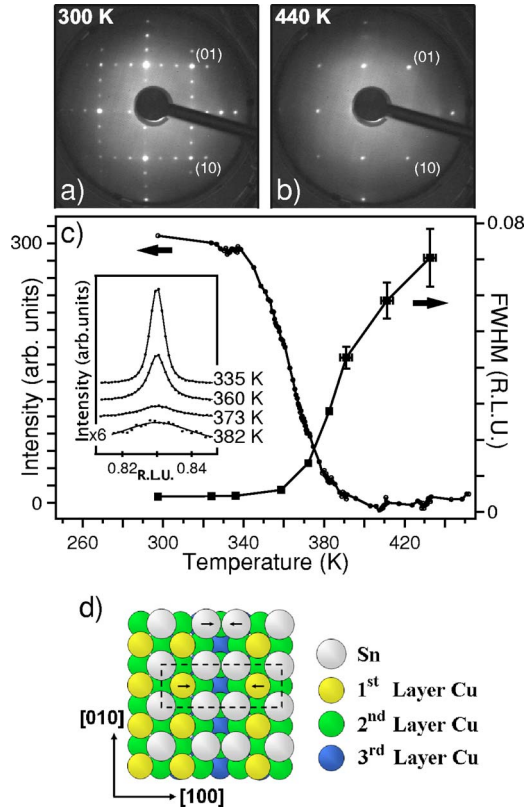


FIG. 1. (Color online) (a) LEED patterns at 70 eV primary energy for 0.53 ML Sn/Cu(100) at (a) 300 and (b) 440 K. (c) Integrated intensity and peak width of the  $(5/6, 5/6)$  x-ray reflection of the  $3\sqrt{2}$  phase vs temperature. The inset shows the reflection fitted with a Lorentzian/Voigt line shape (Ref. 16). (d) Atomic model of the  $3\sqrt{2}$  phase (from Ref. 13).

sequence of structures below 1 ML (Ref. 15) and from the Sn  $5d/\text{Cu } 3d$  intensity ratio measured with  $h\nu=60$  eV. The phase transition is fully reversible. Symmetry points are referred to the Cu(100) surface Brillouin zone, unless otherwise stated.

Figure 1 shows the LEED patterns of the  $3\sqrt{2}$  and the  $\sqrt{2}$  phases, and the atomic model of the  $3\sqrt{2}$  phase from Ref. 13. In this model, the triple periodicity is due to a one-dimensional pairing of Sn atoms along either the  $[100]$  or the  $[010]$  direction, giving rise to the two domains observed in the LEED pattern. Figure 1 shows also the temperature dependence of a superstructure x-ray reflection. Its Debye-Waller corrected intensity (structural order parameter) presents a steep decrease with an inflection point at  $\sim 360$  K, the critical temperature ( $T_c$ ) of the phase transition. Broadened diffraction peaks are observed above  $T_c$ . Their line shape is fitted using a Lorentzian/Voigt.<sup>16</sup> The temperature dependence of the Lorentzian full width at half maximum (FWHM) is shown in Fig. 1. Considering that the mean domain size is  $2\pi/(\text{FWHM})$ , the increase of width reflects the existence of reduced domain sizes down to  $\sim 40$  Å at  $\sim 400$  K. This finding is compared below with the temperature dependence of the electronic structure.

The projection of Cu electronic bulk bands along the  $[001]$  direction leaves an absolute band gap around  $\bar{M}$  points,

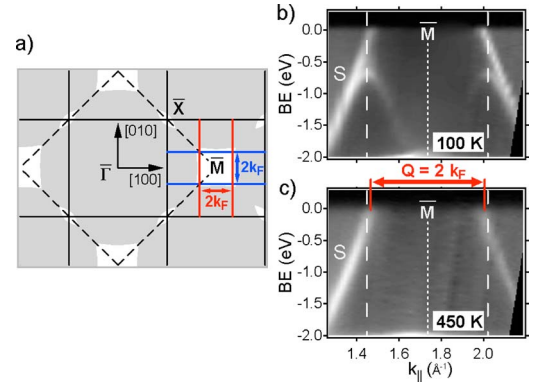


FIG. 2. (Color online) (a) Cu(100) reciprocal space. Unshaded areas denote bulk band gaps. Dashed (continuous) black lines are the surface Brillouin zones of Cu(100) ( $\sqrt{2}$  phase). Red and blue lines (dark gray horizontal and vertical lines) correspond to the  $3\sqrt{2}$  Brillouin zones of each domain. The two  $2k_F$  nesting vectors around  $\bar{M}$  are shown. (b) and (c) Valence-band structure in gray scale with  $h\nu=27$  eV at 100 K ( $3\sqrt{2}$  phase) and 450 K ( $\sqrt{2}$  phase) vs parallel momentum ( $k_{\parallel}$ ), respectively. Vertical dashed lines are the  $3\sqrt{2}$  Brillouin-zone boundaries.

as shown in Fig. 2. ARPES spectra of both phases are measured along  $\bar{\Gamma}\bar{M}$  in the band-gap region. A prominent surface peak  $S$  is observed at 450 K in the  $\sqrt{2}$  phase.<sup>17</sup> The orbital origin of  $S$  is ascribed to a Sn  $5sp$ -Cu  $4sp$  band.<sup>18</sup> Its rapid, parabolic dispersion towards the Fermi energy ( $E_F$ ) indicates a nearly free-electron behavior. It crosses  $E_F$  at  $1.46$  Å<sup>-1</sup> and again at  $2.01$  Å<sup>-1</sup>, the equivalent point beyond  $\bar{M}$ . These two crossing points span a vector  $2k_F=(0.55\pm 0.02)$  Å<sup>-1</sup>. A simple one-band model with parabolic dispersion of the form  $E=E_0+\hbar^2k_{\parallel}^2/2m^*$  reproduces well the experimental surface state, with values of  $E_0=-6.0$  eV (bottom of the band) and  $m^*=1.3m_e$  ( $m_e$ , electron mass). The formation of a  $3\sqrt{2}$  phase below 360 K has dramatic effects in  $S$  [Fig. 2(b)]. In an energy range of  $\sim 0.7$  eV from  $E_F$ , the  $S$  band is split in two different bands. The splitting is explained from the two-domain nature of the  $3\sqrt{2}$  phase. The reciprocal space area probed in Fig. 2 is close to the Brillouin-zone edge for one of the domains, but far away for the other [Fig. 2(a)]. Thus, we detect at the same time a band folding (with the opening of a surface band gap) for one of the domains, and for the other domain, a band which behaves as in the  $\sqrt{2}$  phase. The first band crosses the Fermi energy at  $1.46$  Å<sup>-1</sup>, exactly as for the  $\sqrt{2}$  phase. The second band folds back at  $1.44$  Å<sup>-1</sup>, with a minimum binding energy (BE) of 0.7 eV (at 100 K). The folding point coincides very precisely with the  $3\sqrt{2}$  Brillouin-zone edge at  $1.45$  Å<sup>-1</sup>. Indeed, the  $2k_F$  nesting vector of the  $\sqrt{2}$  phase is equal within  $0.03$  Å<sup>-1</sup> to the periodicity of the  $3\sqrt{2}$  phase ( $0.58$  Å<sup>-1</sup>).

The simultaneous observation of the two bands prevents the detection of an absolute band gap. Nevertheless, this feature provides the unique possibility of probing simultaneously the surface electron band affected and unaffected by the phase transition, i.e., the Fermi energy crossing point (Fermi contour) and the backfolding point. Selected series of ARPES spectra taken along different azimuthal directions are shown in Fig. 3(a). For each azimuthal direction,  $S$

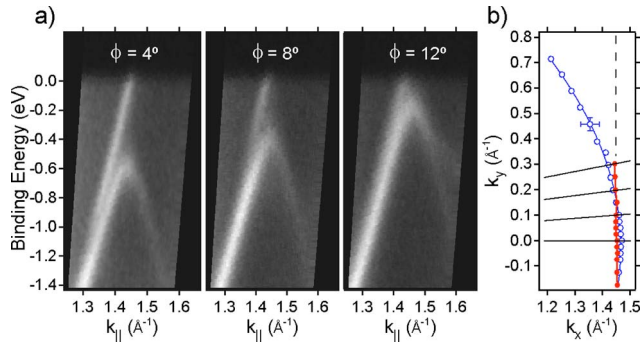


FIG. 3. (Color online) (a) Valence-band structure (in gray scale) at 300 K for selected azimuthal angles with respect to the  $\Gamma M$  direction ( $\phi$ ). A band gap opens as the  $\Gamma M$  direction is approached. (b) High-resolution Fermi contour (open blue circles) and backfolding line (solid red circles). Continuous lines mark the directions used in the plots of panel (a) and  $\Gamma M$  ( $\phi=0^\circ$ ) (shown in Fig. 2). The vertical dashed line is the  $3\sqrt{2}$  zone edge.

crosses  $E_F$  at a different  $k_{||}$  wave vector, defining a point of the  $\sqrt{2}$  ungapped Fermi contour, and a backfolding point in reciprocal space [Fig. 3(b)]. The latter follows very precisely a straight line, which coincides with the  $3\sqrt{2}$  Brillouin-zone boundary. In agreement with the quasi-free-electron character of  $S$ , the Fermi contour is a slightly deformed circle. As long as the Fermi contour coincides with the  $3\sqrt{2}$  Brillouin-zone boundary within  $0.04 \text{ \AA}^{-1}$ , a backfolding and a band gap are observed. This range is close to the  $k$  width of  $S$  ( $\sim 0.04 \text{ \AA}^{-1}$ ), suggesting that the nesting condition is satisfied within this width. The band gap diminishes away from  $\Gamma M$ , as the nesting condition is less perfectly satisfied [see Fig. 3(a)]. It becomes zero at  $\sim 13^\circ$ , as the backfolding disappears. From these and additional data we estimate that approximately 15% of the Fermi surface is gapped in each of the domains of the  $3\sqrt{2}$  phase. These results demonstrate that the phase transition is associated with the partial nesting of the two-dimensional Fermi surface, which gives rise to a momentum-dependent surface band gap in the  $3\sqrt{2}$  phase.

The band-gap thermal behavior is analyzed in Fig. 4. The two peaks observed at 100 K correspond to the crossing point and the backfolding point of  $S$ , close to  $k_{||}=1.44 \text{ \AA}^{-1}$ . As temperature increases, the BE of the backfolding point decreases slowly, indicating that the band gap diminishes accordingly. The value of the band gap (below  $E_F$ ) is obtained from a fitting of the experimental line shape.<sup>19</sup> Panel (b) shows the temperature dependence of the band gap. The band gap (electron order parameter) mimics the behavior of the structural order parameter in Fig. 1, but with an inflection point at  $\sim 400$  K, i.e., clearly above the value of  $T_c$  (360 K). Since relatively large  $3\sqrt{2}$  domains survive above  $T_c$ , we expect that the band gap (associated with the  $3\sqrt{2}$  distortion) also survives.

These results provide information on the nature of the phase transition. The opening of a band gap in a delocalized state, concomitantly with the structural phase transition, and the excellent agreement with the  $2k_F$  nesting condition for a significant fraction of the Fermi surface, suggest that an electronic energy gain plays a crucial role in the phase transition, as it is the case in the stabilization of a CDW. In the Peierls-

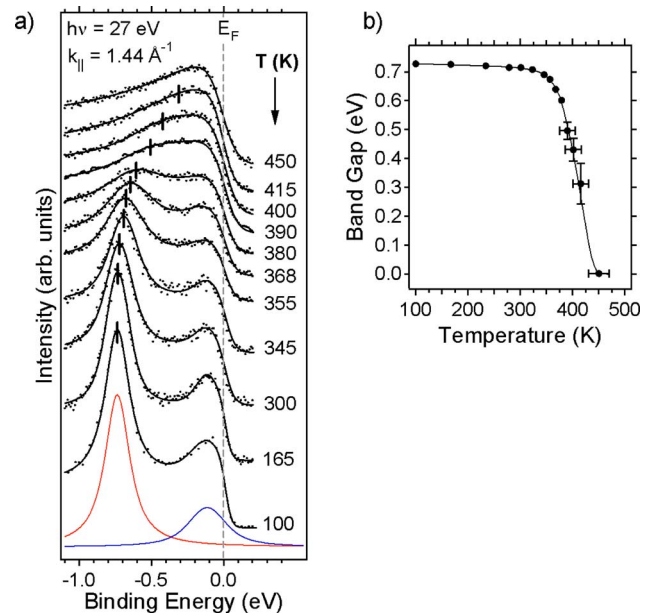


FIG. 4. (Color online) (a) Angle-resolved energy distribution curves (dots) corresponding to  $k_{||}=1.44 \text{ \AA}^{-1}$  as a function of temperature. Continuous lines are a fit to the data (see text). The two components used (red-light gray and blue-dark gray) are shown at 100 K. Tics mark the position of the backfolded band (band gap). The band gap below  $E_F$  vs temperature is shown in panel (b). The continuous line is a guide to the view.

Fröhlich theory of a CDW (Refs. 10–12),  $2W=3.5k_B T_c$ . For Sn/Cu(100), the value of  $2W/k_B T_c$  is  $\sim 45$ , typical of the strong electron-phonon coupling limit.<sup>1,10,20–22</sup> Due to this reason, the band gap may survive up to a temperature  $T_0$  much larger than the critical temperature  $T_c$  (Refs. 20 and 21). In the range  $T_c < T < T_0$  fluctuations destroy long-range order in a strong-coupling CDW, but there is enough local coherence to observe the band gap. In the case of Sn/Cu(100), the band gap goes to zero only  $\sim 40$  K above the structural critical temperature  $T_c$ , indicating that this order-disorder regime is narrow, and that the gain in electronic energy is indeed driving the phase transition. This is in agreement with the excellent nesting behavior found. We note that the existence of an order-disorder intermediate regime is not incompatible with a displacive character for the phase transition.<sup>23</sup> The question whether the  $\sqrt{2}$  phase is disordered or not requires an analysis of the structure and the dynamical behavior (phonon structure) across the phase transition, and is beyond the scope of this paper. We conclude that a gain in electronic energy is behind the formation of the  $3\sqrt{2}$  phase, which can be interpreted as a surface CDW. Detailed information on the nature of the atomic displacements across the phase transition is needed to confirm this assignment.

We compare now the two systems Sn/Cu(100) and In/Cu(100) for 0.5 ML adsorbate.<sup>7</sup> In a quasi-free-electron two-dimensional band, the value of  $k_F$  is simply related to the electronic density  $n_{2D}$  as  $k_F=\sqrt{2\pi n_{2D}}$ , which gives a value of  $3.4 \times 10^{15}$  electrons/cm<sup>2</sup>, equivalent to  $\sim 4.4$  electrons per  $\sqrt{2}$  unit cell. A similar value for  $n_{2D}$  is reached from  $m^*$  and  $E_0$ . In spite of the fact that Sn has one more electron

than In, the value of  $k_F$  is equal within experimental accuracy in both systems ( $1.46 \text{ \AA}^{-1}$  for Sn versus  $1.44 \text{ \AA}^{-1}$  for In). Furthermore, the close values of the critical temperatures and the band gap indicate that the electronic energy involved in the transition is similar in both cases. These facts support a main role of the substrate. We conclude that the Cu(100) surface is prone to an instability, which is triggered by an adsorbate layer. This is a feature with potential implications in other Cu-based structures. However, each interface reacts in a different way below  $T_c$ . In the case of In/Cu(100) a more complex  $(9\sqrt{2} \times 2\sqrt{2})R45^\circ$  structure is found, with maximum gapping at the edges of the  $\sqrt{2}$  Fermi surface,<sup>7</sup> and with a nesting vector which does not directly correspond to the surface periodicity. On the contrary, in the case of Sn/Cu(100) the surface structure reflects neatly the electronic periodicity and the gapping is maximum at the optimal nesting areas. This shows the importance of the electronic energy in determining the properties of the phase transition for Sn/Cu(100).

In summary, we report a reversible surface phase transition in Sn/Cu(100). Below the phase transition, a large gap opens in optimally nested regions of the Fermi surface, while areas with poorer nesting remain ungapped. We conclude that the  $3\sqrt{2}$  phase is stabilized by a gain in electronic energy related with the Fermi energy gapping, and it can be understood as a charge-ordered state. This phase transition presents a clear experimental phenomenology, which makes it an easily accessible experimental system to test paradigms such as Fermi gap stabilization and its role in CDW formation in 2D systems.

We acknowledge financial support by the Spanish MEC (BFM2001-0244 and “Ramón y Cajal” Program) and by UAM-SCH. Work at MaxLab and Elettra is supported by the EC-Research Infrastructure Action under the FP6 “Structuring the European Research Area” Program (through the Integrated Infrastructure Initiative “Integrating Activity on Synchrotron and Free Electron Laser Science”).

- 
- <sup>1</sup>E. Tosatti, *Electronic Surface and Interface States on Metallic Systems*, edited by E. Bertel and M. Donath (World Scientific, Singapore, 1995).
- <sup>2</sup>M. K. Debe and D. A. King, *J. Phys. C* **10**, L303 (1977); C. Binns, M. G. Barths-Labrousse, and C. Norris, *ibid.* **17**, 1465 (1984); F. M. Hoffmann, B. N. J. Persson, W. Walter, D. A. King, C. J. Hirschmugl, and G. P. Williams, *Phys. Rev. Lett.* **72**, 1256 (1994); E. Hulpke and J. Lüdecke, *ibid.* **68**, 2846 (1992).
- <sup>3</sup>A. Mascaraque, J. Avila, J. Alvarez, M. C. Asensio, S. Ferrer, and E. G. Michel, *Phys. Rev. Lett.* **82**, 2524 (1999).
- <sup>4</sup>J. Avila, A. Mascaraque, E. G. Michel, M. C. Asensio, G. LeLay, J. Ortega, R. Pérez, and F. Flores, *Phys. Rev. Lett.* **82**, 442 (1999).
- <sup>5</sup>H. W. Yeom, S. Takeda, E. Rotenberg, I. Matsuda, K. Horikoshi, J. Schaefer, C. M. Lee, S. D. Kevan, T. Ohta, T. Nagao, and S. Hasegawa, *Phys. Rev. Lett.* **82**, 4898 (1999).
- <sup>6</sup>K. Swamy, A. Menzel, R. Beer, and E. Bertel, *Phys. Rev. Lett.* **86**, 1299 (2001).
- <sup>7</sup>T. Nakagawa, G. I. Boishin, H. Fujioka, H. W. Yeom, I. Matsuda, N. Takagi, M. Nishijima, and T. Aruga, *Phys. Rev. Lett.* **86**, 854 (2001); T. Nakagawa, S. Mitsushima, H. Okuyama, M. Nishijima, and T. Aruga, *Phys. Rev. B* **66**, 085402 (2002).
- <sup>8</sup>T. Nakagawa, H. Okuyama, M. Nishijima, T. Aruga, H. W. Yeom, E. Rotenberg, B. Krenzer, and S. D. Kevan, *Phys. Rev. B* **67**, 241401(R) (2003).
- <sup>9</sup>F. Schiller, J. Cerdón, D. Vyalikh, A. Rubio, and J. E. Ortega, *Phys. Rev. Lett.* **94**, 016103 (2005).
- <sup>10</sup>G. Grüner, *Density Waves in Solids* (Addison-Wesley, Reading, MA, 1994).
- <sup>11</sup>R. E. Peierls, *Quantum Theory of Solids* (Clarendon, Oxford, 1955).
- <sup>12</sup>A. Fröhlich, *Proc. R. Soc. London, Ser. A* **233**, 296 (1954).
- <sup>13</sup>K. Pussi, E. AlShamaileh, E. McLoughlin, A. A. Cafolla, and M. Lindroos, *Surf. Sci.* **549**, 24 (2004).
- <sup>14</sup>The total energy resolution in BL 33 (APE) was 60 meV (50 meV) and the angular resolution was  $\pm 0.5^\circ$  ( $\pm 0.12^\circ$ ).
- <sup>15</sup>E. McLoughlin, A. A. Cafolla, E. AlShamaileh, and C. J. Barnes, *Surf. Sci.* **482–485**, 1431 (2001).
- <sup>16</sup>The two domains below the phase transition generate a Voigt line shape. The Gaussian contribution is marginal.
- <sup>17</sup>The surface character of  $S$  is checked also by varying the photon energy in the range 21–70 eV.
- <sup>18</sup>X. Gao, Y. M. Zhou, S. C. Wu, and D. S. Wang, *Phys. Rev. B* **66**, 073405 (2002).
- <sup>19</sup>We use a Shirley background and two Voigt components, convoluted with a Fermi function.
- <sup>20</sup>W. L. McMillan, *Phys. Rev. B* **16**, 643 (1977).
- <sup>21</sup>C. M. Varma and A. L. Simons, *Phys. Rev. Lett.* **51**, 138 (1983).
- <sup>22</sup>A. Fournel, J. P. Sorbier, M. Konczykowski, and P. Monceau, *Phys. Rev. Lett.* **57**, 2199 (1986).
- <sup>23</sup>H. J. Ernst, E. Hulpke, and J. P. Toennies, *Phys. Rev. B* **46**, 16081 (1992).